Structural Engineering and Mechanics, *Vol. 59, No. 4 (2016) 621-652*
DOI: http://dx.doi.org/10.12989/sem.2016.59.4.621

Economic performance of cable supported bridges

Bin Sun*, Liwen Zhang, Yidong Qin and Rucheng Xiao

Department of Bridge Engineering, Tongji University, 1239 Siping Rd., Shanghai 200092, China

(Received December 17, 2015, Revised May 20, 2016, Accepted June 10, 2016)

Abstract. A new cable-supported bridge model consisting of suspension parts, self-anchored cable-stayed parts and earth-anchored cable-stayed parts is presented. The new bridge model can be used for suspension bridges, cable-stayed bridges, cable-stayed suspension bridges, and partially earth-anchored cable-stayed bridges by varying parameters. Based on the assumption that each structural member is in either an axial compressive or tensile state, and the stress in each member is equal to the allowable stress of the material, the material quantity for each component is calculated. By introducing the unit cost of each type of material, the estimation formula for the cost of the new bridge model is developed. Numerical examples show that the results from the estimation formula agree well with that from the real projects. The span limit of cable supported bridge depends on the span-to-height ratio and the density-to-strength ratio of cables. Finally, a parametric study is illustrated aiming at the relations between three key geometrical parameters and the cost of the bridge model. The optimization of the new bridge model indicates that the self-anchored cable-stayed part is always the dominant part with the consideration of either the lowest total cost or the lowest unit cost. It is advisable to combine all three mentioned structural parts in super long span cable supported bridges to achieve the most excellent economic performance.

Keywords: cable supported bridge; new bridge model; cost estimation formula; material quantity; unit cost; span limit; parametric study; geometrical parameters; geological conditions

1. Introduction

Cable supported bridges, including suspension bridges (SB) and cable-stayed bridges (CSB), are mainly used for bridges with a main span over 600 m. Some new cable supported bridge types, such as cable-stayed suspension bridge (CSSB) and partially earth-anchored cable-stayed bridge (PEACSB), have been proposed to possibly extend the span limit of bridges since the 1980's (Gimsing and Georgakis 2012, Nagai *et al*. 2004, Sun *et al*. 2010, Tang 2007, Shao *et al*. 2013).

For a new bridge design, the first step is to choose a right bridge type. On the premise to meet the navigation requirement, a better economic performance usually is preferred other than a larger span. Therefore, it is necessary to have a better estimation and optimization of the total bridge cost. However, in most projects, especially in either the conceptual design or preliminary design process, the cost is usually estimated simply based on either the experiences from previous similar project or the unit cost per deck area. Only a few studies focusing on the mathematical model of

*Corresponding author, Lecturer, E-mail: sunbin@tongji.edu.cn

http://www.techno-press.org/?journal=sem&subpage=8 ISSN: 1225-4568 (Print), 1598-6217 (Online)

bridge's cost are found in literature.

Recently, some studies have aimed at the optimization of either the total material quantity or cost of the bridge by using advanced numerical methods, such as genetic algorithms (GA). For example, Lute *et al*. (2009) adopted a new approach combining GA and support vector machine (SVM) to reduce the computation time to obtain the minimum cost of CSB. Hassan *et al*. (2013) developed a numerical design tool integrating a finite element model, GA, and simple polynomial functions to optimize the steel weight of the stay cables in CSB, and Hassan *et al*. (2014) extended their work by developing a database for the optimum design parameters. They defined the geometric configuration and cross-sectional dimensions of various components for semi-fan composite CSB.

However, all these methods could not study the effects of the structural parameters on the bridge's cost in an analytical way. Instead, they need a large number of calculation results to perform the regression analysis. Therefore, the structural parameters' effects on the cost are still implicit.

For a better understanding of a bridge's cost and the influencing rules, many analytical methods for calculating the material quantity and the associated cost are proposed as well. Gimsing (2012) derived the expressions for the quantities and costs of the cable steel and pylon in three types of cable-supported bridges, including SB, the fan-type CSB, and the harp-type CSB. These expressions are based on the assumptions that all components are subjected to axial force, and that all of the materials reach their allowable stresses under the imposed loads. Gimsing also found that the optimum ratio of the pylon's height to the mid span length was about 0.17 for SB and fan type CSB with steel girder, and 0.25 for those with concrete girder. The doubled values of 0.34 and 0.50 were recommended for harp type CSB. Meanwhile, Lewis (2012) presents a refined mathematical model for the assessment of relative material costs of the supporting structures for CSB and SB. The proposed model is more accurate than the old ones in that it includes the self-weight of the cables and the pylons. The optimum height-to-span ratio was derived as 1/5 for SB, and 1/3 for the harp type CSB. However, in both models from Gimsing and Lewis, the quantities and costs are considered only within the cables and pylons, while those for the anchorages and foundations are not considered, though they occupy a large portion of the total cost of a cable-supported bridge. Later on, Zhang *et al*. (2013 a, b) studied the economic performances of consecutive multi-span SB by deriving the formulas for the material quantity and the cost estimation that could include all of the structural components of the bridges. However, CSB were not included. Recently, Zhang *et al.* (2014) also presented a series of formulas for material cost of CSSB based on the allowable stress design method. Until now, all discussions are within specific bridge types, including CSB, SB, and CSSB. This means that different bridge models and several series of expressions are needed for proper bridge types. If a new type of composite cable supported bridge is considered, for example, PEACSB, the research must start all over again, and the expressions would be in other forms.

On the other hand, the life-cycle cost is a new concept for bridge engineering in recent years, aiming to determine the most cost-efficient option from the inception to the disposal of a structure. Eamon *et al.* (2012) conducted on prestressed concrete bridge superstructures using carbon fiber reinforced polymer (CFRP) material and found that although more expensive initially, the use of CFRP reinforcement has the potential to achieve significant reductions in life-cycle cost. Thoft-Christensen (2012) discussed the design and maintenance of infrastructures using life-cycle cost-benefit analysis with special emphasis on users' costs. Mara *et al.* (2013) conducted a life-cycle cost analysis and concluded that two steel-fiber reinforced polymer (FRP) bridge alternatives were competitive in terms of costs and environmental impacts compared with the conventional bridge option. Wang *et al*. (2015) summarized the major hazards of in-service cable supported bridges and introduced advanced maintenance and rehabilitation tools to save the life-cycle cost. However, the life-cycle cost is highly related to the durability of the materials and the maintenance strategies. This study focuses on the cost in terms of material quantities through structural analysis. Thus, the life-cycle cost is beyond the scope of this study and not discussed hereafter.

In this study, a rigorous mathematical model for predicting the cost of cable-supported bridges is developed. The cable-supported bridge model includes the suspension parts, self-anchored cable-stayed parts, and earth-anchored cable-stayed parts, and it can be degraded to all of the formerly mentioned bridge types by using different parameters. Therefore, the economic performance for all types of the cable-supported bridges could be investigated and compared.

In order to decrease the total cost of the bridge, new materials besides concrete and steel with higher strength have been proposed for new designs. To this end, the economic performance of fiber reinforced polymer (FRP) has been carried out. Wang and Wu (2010 a, b) found that the hybrid FRP cables with a proper volume proportion of carbon fibers and the FRP cables would exhibit a superior performance/cost ratio even within a 3000m main span. Xiong *et al*. (2013) introduced new types of CSB with carbon FRP (CFRP) stay cables and/or a CFRP bridge deck. The results indicated that CSB using CFRP materials still cost more than the traditional designs based on the current price of CFRP materials. However, the economic benefit of using CFRP components with possible savings on the material quantity can be definitely shown in the near future with the continuous drop of the cost for CFRP materials. Therefore, the FRP and its comparison with steel are included in the present study, even though it has never been practically applied in any long span CSB yet.

In the present study, the material quantity for each structural component, including the cable, the pylon, the girder, the anchorage, and the foundation, is calculated based on the assumption that each structural member is in either an axial compressive or tensile state, and the stress in each member is equal to the allowable stress of the material. In the cable-stayed parts, the additional material quantity for the girder due to the accumulated axial force is included, as well. By introducing the unit cost of each type of material, the formula for the total cost of the bridge is easily obtained. Numerical examples show that the estimation formula agrees well with practice. Then, the theoretical span limits of SB and CSB are obtained based on the condition that the cables can only sustain their self-weight.

After that, a parametric study is performed focusing on several selected key parameters. Due to the complexity of the new bridge model, three important concepts are introduced. Firstly, most parameters are studied in particular degraded bridge types in which the parameters exist. Secondly, besides the key parameter being discussed, the rest parameters take the values corresponding to the lowest cost; otherwise the values are specially mentioned. Lastly but not the least, both total cost and unit cost per deck area are discussed, and mostly the results are quite different. For a given length of the mid-span, minimizing the total length is beneficial for the total cost, but it is just on the contrary for the unit cost. That is the reason for the different optimal values for the same parameter.

2. New model for cable-supported bridges

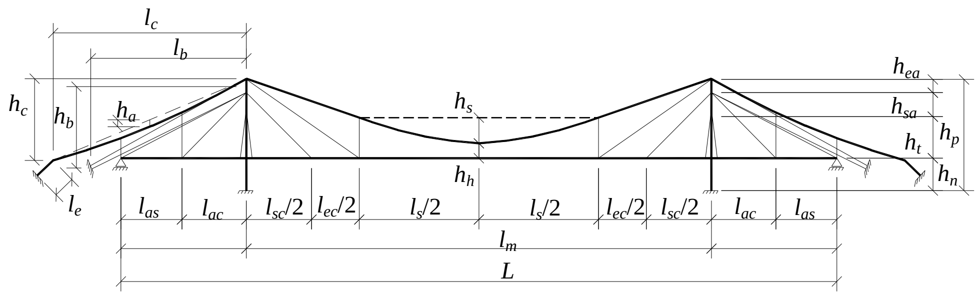

Fig. 1 New bridge model

In order to investigate the economic performance of cable-supported bridges, a new cable-supported bridge model, which can cover all types of the existing cable-supported bridge with only one main span, is established as shown in Fig. 1. The model could be used for all of the four cable-supported bridge types, cable-stayed bridges, suspension bridges, PEACSBs and CSSBs, by using different geometrical parameters.

The new bridge model can be divided into five parts: the cable system, the girders, the pylons, the anchorages and the foundations. The cable system consists of self-anchored stay cables, earth-anchored stay-cables, hangers and main cables. The girder in the mid span comprises self-anchored cable-stayed parts with the total length of l_{sc}, earth-anchored cable-stayed parts with the total length of l_{ec}, and a suspension part with the length of l_s. The girder in each side span comprises a self-anchored cable-stayed part with the length of l_{ac}, and a suspension part with the length of l_{as}. Two pylons, each with a total height of h_p, are included in the model. The anchorages include those fixing the main cables and those fixing the earth-anchored stay cables. The foundations include the piers with the foundations below them and the pylon foundations. These foundations bear the total weight of the bridge. They are seen as a whole part regardless of the locations in this study.

3. Material quantity and cost estimation formulas

3.1 Fundamental approach

The fundamental assumptions in this study are as follows:

• Each structural part in Fig. 1 and mentioned in part 2 is mainly subjected to the axial force (Gimsing 2012, Lewis 2012). And only zigzagged bending moment exists along the girder. (Hassan *et al* 2013, Sun *et al* 2010).

• Only the self-weight of the structures and a uniformly distributed live load along the girder are taken into account in the calculation of the axial force. Commonly, the live loads in design codes in most countries are composed of a uniformly distributed load and several concentrated loads. In long span bridges, especially in conceptual design stage, the concentrated loads can be safely divided into a uniformly distributed live load thus the live load could be safely represented with only a uniformly distributed live load.

• The material quantity for each structural component is obtained with the assumption that the stress reaches the allowable stress of the material.

• The possible bending moment is taken into account with a safety factor in the allowable stress of the material.

Therefore, the material quantity Q for each component, the total cost C and the cost per unit deck area C_u are calculated with Eq. (1)-(3), respectively.

$$Q_i = \frac{\gamma_i}{f_i} N_i l_i \tag{1}$$

$$C = \sum_{i=1}^{n} \mu_i Q_i \tag{2}$$

$$C_u = C / (BL) \tag{3}$$

where γ is the density of the material, f is the allowable stress of the material, N is the axial force, l is the length of the structural component, μ is the unit cost of the material, B is the deck width, L is the total length of the bridge, and i is the i^{th} structural component, which will be replaced by a, c, f, g, h, p, and s representing the anchorages, stay cables, foundations, girders, hangers, pylons and main cables, respectively.

The material quantity Q is calculated in only one half of the bridge because of the symmetry, and they will be doubled in section 3.5.

3.2 Cable system

3.2.1 Mid-span hangers

The parabola shape is adopted for the main cable in the suspension part l_s, and the hangers are assumed as a continuous cable membrane as shown in Fig. 2.

A differential equation for the vertical tensile force in the differential membrane element is established as follows

$$\mathrm{d}T = \left(g_s + g_2 + p\right)\mathrm{d}x + \gamma_h \left(h_h + \frac{4h_s}{l_s^2} x^2\right)\mathrm{d}A \tag{4}$$

where g_s is the uniform weight of girder in the suspension part in the mid span; g_2 is the uniformly

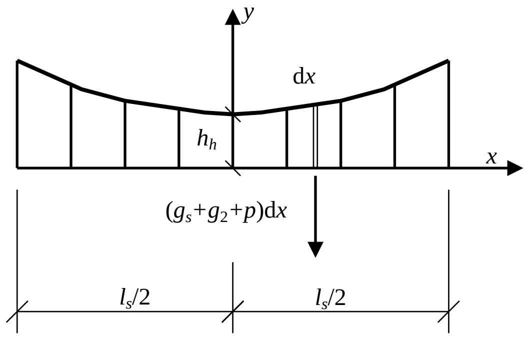

Fig. 2 Force in hangers

superimposed dead load along all of the girders in the bridge, accounting for pavement, handrail, curb, and attachment, etc.; p is the uniformly distributed live load; h_h is the distance from the girder to the main cable at the bridge center, and h_s is the cable sag in the mid-span suspension part.

By taking dT=f_hdA into Eq. (4), dA is expressed as

$$\mathrm{d}A = \frac{g_s + g_2 + p}{f_h - \gamma_h\left(h_h + \frac{4h_s}{l_s^2}x^2\right)}\mathrm{d}x \tag{5}$$

Then, the material quantity for the hanger in the mid-span Q_{hm} can be derived through the integration of Eq. (5), as shown in Eq. (6)

$$Q_{hm} = \int_{l_s/2} \gamma_h (h_h + \frac{4h_s}{l_s^2}x^2)\mathrm{d}A = (g_s + g_2 + p)\frac{l_s}{2}\left\{\frac{f_h}{2\sqrt{(f_h - \gamma_h h_h)\gamma_h h_s}}\ln\frac{\sqrt{f_h - \gamma_h h_h} + \sqrt{\gamma_h h_s}}{\sqrt{f_h - \gamma_h h_h} - \sqrt{\gamma_h h_s}} - 1\right\} \tag{6}$$

If the self-weight of the hangers expressed with the second item in Eq. (4) is ignored, Q_{hm} can be simplified as

$$Q_{hm} = \frac{\gamma_h}{f_h}(g_s + g_2 + p)(h_h + \frac{h_s}{3})\frac{l_s}{2} \tag{7}$$

3.2.2 Side-span hangers

A straight line shape is adopted for the main cable in the side span considering that the sag h_a is very small compared with h_s. Therefore, Eq. (4) is transformed into $dT = f_h dA = \left(g_{as} + g_2 + p\right)dx + \gamma_h[h_p - h_c(l_a - x)/l_c]dA$, and Eq. (5) is transformed into $dA = (g_{as} + g_2 + p)dx/\{f_h - \gamma_h[h_p - h_c(l_a - x)/l_c]\}$, respectively. The material quantity for side-span hangers Q_{ha} can be obtained according to the same method for the mid-span hangers in the former section. Thus, Q_{ha} is expressed as

$$Q_{ha} = (g_{as} + g_2 + p)\left(\frac{f_h}{\gamma_h}\frac{l_c}{h_c}\ln\frac{f_h l_c - \gamma_h h_{po} l_c + \gamma_h h_c l_a}{f_h l_c - \gamma_h h_{po} l_c + \gamma_h h_c l_{ac}} - l_{as}\right) \tag{8}$$

where g_{as} is the uniform weight of the girder in the side-span suspension part; l_c and h_c are the horizontal and vertical projection length of main cable in the side span, respectively; and h_{po} is the pylon's height over the girder.

If the self-weight of the hangers is ignored, Eq. (8) can be simplified as

$$Q_{ha} = \frac{\gamma_h}{f_h}(g_{as} + g_2 + p)(h_{po} - \frac{l_a - l_{as}/2}{l_c}h_c)l_{as} \tag{9}$$

3.2.3 Mid-span main cable

The horizontal force H_s and the maximum axial force T_s (at the pylon's top) of the main cable is expressed in Eq. (10) and Eq. (11), respectively.

$$H_s = (g_s + g_2 + g_{s1} + g_{h1} + p) l_s^2 / (8h_s) \tag{10}$$

$$T_s = \frac{(g_s + g_2 + g_{s1} + g_{h1} + p) l_s}{8 h_s / l_s} \sqrt{1 + (\frac{4h_s}{l_s})^2} \tag{11}$$

where g_{s1} is the self-weight of the main cable in the mid span, and g_{h1} is the hangers' uniform weight.

By replacing $T_s{=}A_s f_s$, $g_{s1}{=}A_s\gamma_s$, and $g_{h1}{\approx}Q_{hm}/(l_s/2)$ into Eq. (11), the cross-sectional area of the main cable A_s is obtained as Eq. (12)

$$A_s = \frac{(g_s + g_2 + g_{h1} + p) l_s}{8 f_s \frac{h_s}{l_s} - \gamma_s l_s \sqrt{1 + (\frac{4h_s}{l_s})^2}} \sqrt{1 + (\frac{4h_s}{l_s})^2} \tag{12}$$

Then the material quantity for the main cable in the main span Q_{sm} can be calculated by multiplying A_s and the cable's length as shown in Eq. (13). The cable's length includes two parts: the parabola's length in the suspension part as $1 + 8(h_s/l_s)^2/3$ and the straight lines' length in the cable-stayed parts as $(l_{ec} + l_{sc})\sqrt{1 + (4h_s/l_s)^2} \,/\, l_s$.

$$Q_{sm} = \frac{\gamma_s}{2 f_s} \frac{(g_s + g_2 + 2Q_{hm}/l_s + p) l_s^2}{\frac{8h_s}{l_s} - \frac{\gamma_s}{f_s} l_s \sqrt{1 + \left(\frac{4h_s}{l_s}\right)^2}} \left[1 + \frac{8}{3}(\frac{h_s}{l_s})^2 + \frac{l_{ec} + l_{sc}}{l_s} \sqrt{1 + \left(\frac{4h_s}{l_s}\right)^2} \right] \sqrt{1 + \left(\frac{4h_s}{l_s}\right)^2} \tag{13}$$

If the self-weight of the main cable is ignored, Eq. (13) can be simplified as

$$Q_{sm} = \frac{\gamma_s}{2 f_s} \frac{(g_s + g_2 + p) l_s^2}{8 h_s / l_s} \left[1 + \frac{8}{3}(\frac{h_s}{l_s})^2 + \frac{l_{ec} + l_{sc}}{l_s} \sqrt{1 + \left(\frac{4h_s}{l_s}\right)^2} \right] \sqrt{1 + \left(\frac{4h_s}{l_s}\right)^2} \tag{14}$$

3.2.4 Side-span main cable

Considering that the horizontal force along the main cable in the side span is equal to that in the main span, the sag of side-span main cable h_a should be

$$h_a = \frac{M_{ha}}{H_s} \tag{15}$$

where M_{ha} is the bending moment at the middle point in the equivalent simply supported beam with the same loads and horizontal span as the main cable in the side span.

M_{ha} can be expressed as follows considering different situations

$$\begin{cases} M_{ha} = \frac{1}{2}(g_{as} + g_2 + p + Q_{ha}/l_{as}) l_{as} (l_c - \frac{1}{2} l_{as} - l_{ac}) & (\frac{1}{2} l_c < l_{ac}) \\ M_{ha} = \frac{1}{2}(g_{as} + g_2 + p + Q_{ha}/l_{as})(l_{as} l_c + l_{ac} l_c - \frac{1}{2} l_{as}^2 - l_{ac}^2 - l_{as} l_{ac} - \frac{1}{4} l_c^2) & (l_{ac} < \frac{1}{2} l_c < l_a) \\ M_{ha} = \frac{1}{2}(g_{as} + g_2 + p + Q_{ha}/l_{as}) l_{as} (\frac{1}{2} l_{as} + l_{ac}) & (l_a < \frac{1}{2} l_c) \end{cases} \tag{16}$$

Then, the maximum axial force T_a and material quantity for the side-span main cable Q_{sa} is calculated with Eq. (17) and Eq. (18), respectively

$$T_a = \frac{\left(g_s + g_2 + g_{s1} + g_{h1} + p\right) l_s}{8 h_s / l_s} \sqrt{1 + \frac{(h_c + 4h_a)^2}{l_c^2}} \tag{17}$$

$$Q_{sa} = \frac{\gamma_s}{f_s} \frac{\left(g_s + g_2 + 2Q_{sm}/l_m + 2Q_{hm}/l_s + p\right) l_s l_c}{8 h_s / l_s} \sqrt{1 + \frac{(h_c + 4h_a)^2}{l_c^2}} \left[1 + \frac{1}{2}(\frac{h_c}{l_c})^2 + \frac{8}{3}(\frac{h_a}{l_c})^2 + \frac{l_e}{l_c}\right] \tag{18}$$

where l_e is the main cable length beyond the splay saddle.

If the self-weight of main cable is ignored, the material quantity Q_{sa} can be simplified as

$$Q_{sa} = \frac{\gamma_s}{f_s} \frac{\left(g_s + g_2 + p\right) l_s l_c}{8 h_s / l_s} \sqrt{1 + \frac{(h_c + 4h_a)^2}{l_c^2}} \left[1 + \frac{1}{2}(\frac{h_c}{l_c})^2 + \frac{8}{3}(\frac{h_a}{l_c})^2 + \frac{l_e}{l_c}\right] \tag{19}$$

3.2.5 Mid-span self-anchored stay cables

The mid-span self-anchored stay cable is also assumed as a continuous cable membrane between the girder and the pylon in the region of $l_{sc}/2$ and h_{as} as shown in Fig. 3.

Taking the self-weight of stay cables into account, dN is expressed as

$$\mathrm{d}N = \left[(g_{sc} + g_2 + p)\mathrm{d}x + \frac{\gamma_c}{f_c} l \mathrm{d}N\right] \frac{l}{h_t + 2 h_{sa} x / l_{sc}} \tag{20}$$

Eq. (20) is converted to Eq. (21) after a transposition and a further approximation calculus

$$\mathrm{d}N = \frac{(g_{sc} + g_2 + p) l}{h_t + 2 h_{sa} x / l_{sc}} \mathrm{d}x \Bigg/ \left[1 - \frac{\gamma_c l^2}{f_c (h_t + 2 h_{sa} x / l_{sc})}\right] \approx \frac{(g_{sc} + g_2 + p) l}{h_t + 2 h_{sa} x / l_{sc}} \left[1 + \frac{\gamma_c l^2}{f_c (h_t + 2 h_{sa} x / l_{sc})}\right] \mathrm{d}x \tag{21}$$

where l is the length of the differential membrane element, and it is equal to $(x^2+(h_t+2h_{sa}x/l_{sc})^2)^{1/2}$.

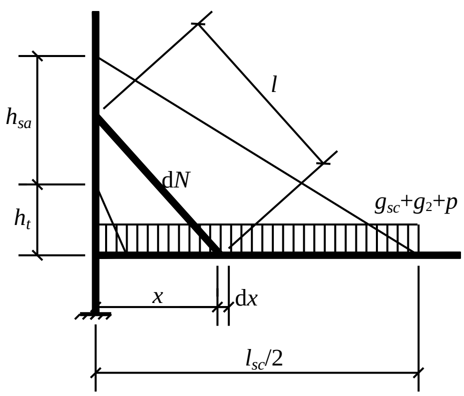

Fig. 3 Axial force in stay cables

Then, the material quantity for the mid-span self-anchored stay cable Q_{sc} is calculated with the following equation

$$Q_{sc} = \frac{\gamma_c}{f_c}(g_{sc} + g_2 + p)(\frac{l_{sc}}{2})^2 \\ \left\{\frac{\gamma_c l_{sc}}{2f_c}(\frac{l_{sc}}{2h_{sa}})^2(\frac{h_t}{h_{sa}})^3\left[1 - 4\ln(1+\frac{h_{sa}}{h_t}) - \frac{1}{1+h_{sa}/h_t} + \frac{3h_{sa}}{h_t} - (\frac{h_{sa}}{h_t})^2 + \frac{1}{3}(\frac{h_{sa}}{h_t})^3\right]\right. \\ + \frac{l_{sc}}{2h_{sa}}(\frac{h_t}{h_{sa}})^2\left[\ln(1+\frac{h_{sa}}{h_t}) - \frac{h_{sa}}{h_t} + \frac{1}{2}(\frac{h_{sa}}{h_t})^2 + \frac{2\gamma_c h_{sa}}{3f_c}(\frac{h_{sa}}{h_t})^2\right] \\ \left. + \frac{2h_t}{l_{sc}}\frac{h_t}{h_{sa}}\left[\frac{\gamma_c h_{sa}}{f_c} + \frac{h_{sa}}{h_t} + \frac{\gamma_c h_{sa}}{f_c}\frac{h_{sa}}{h_t} + \frac{1}{2}(\frac{h_{sa}}{h_t})^2 + \frac{\gamma_c h_{sa}}{3f_c}(\frac{h_{sa}}{h_t})^2\right]\right\} \tag{22}$$

Additionally, the cable-stayed part approaches to either a fan type system or a harp type system when h_{sa} or h_t is approaching to zero, and Eq. (22) is simplified as

$$Q_{sc} = \frac{\gamma_c}{f_c}(g_{sc} + g_2 + p)h_t^2\left[\frac{1}{5}\cdot\frac{\gamma_c l_{sc}}{2f_c}(\frac{l_{sc}}{2h_t})^4 + \frac{1}{3}(1+\frac{2\gamma_c h_t}{f_c})(\frac{l_{sc}}{2h_t})^3 + (1+\frac{\gamma_c h_t}{f_c})\frac{l_{sc}}{2h_t}\right] \quad (h_{sa} = 0) \tag{23}$$

$$Q_{sc} = \frac{\gamma_c}{f_c}(g_{sc} + g_2 + p)(\frac{l_{sc}}{2})^2(\frac{l_{sc}}{2h_{sa}} + \frac{2h_{sa}}{l_{sc}})\left[\frac{1}{2} + \frac{\gamma_c l_{sc}}{6f_c}(\frac{l_{sc}}{2h_{sa}} + \frac{2h_{sa}}{l_{sc}})\right] \quad (h_t = 0) \tag{24}$$

Eq. (23) and (24) are the same as the results of Gimsing (2012) through separate calculations especially for the fan type cable system and the harp type cable system.

If the self-weight of stay cables is ignored, Eq. (22) - (24) can be simplified as

$$Q_{sc} = \frac{\gamma_c}{f_c}(g_{sc} + g_2 + p)(\frac{l_{sc}}{2})^2\left\{\frac{2h_t + h_{sa}}{l_{sc}} + \frac{l_{sc}}{2h_{sa}}(\frac{h_t}{h_{sa}})^2\left[\ln(1+\frac{h_{sa}}{h_t}) - \frac{h_{sa}}{h_t} + \frac{1}{2}(\frac{h_{sa}}{h_t})^2\right]\right\} \tag{25}$$

$$Q_{sc} = \frac{\gamma_c}{f_c}(g_{sc} + g_2 + p)(\frac{l_{sc}}{2})^2(\frac{2h_t}{l_{sc}} + \frac{l_{sc}}{6h_t}) \tag{26}$$

$$Q_{sc} = \frac{\gamma_c}{f_c}(g_{sc} + g_2 + p)(\frac{l_{sc}}{2})^2(\frac{h_{sa}}{l_{sc}} + \frac{l_{sc}}{4h_{sa}}) \tag{27}$$

3.2.6 Side-span self-anchored stay cables

The material quantity s for side-span self-anchored stay cables Q_{ac} can be obtained by replacing $l_{sc}/2$ with l_{ac} and replacing g_{sc} with g_{ac} in Eq. (22)-(27). The result is intentionally omitted.

3.2.7 Mid-span earth-anchored stay cables

The material quantity for mid-span earth-anchored stay cables Q_{ec}, however, is calculated by subtracting the material quantity for the "small" cable membrane in the $l_{sc}/2$ region from that of the "big" cable membrane in the ($l_{sc}/2$+$l_{ec}/2$) region. Eq. (22)-(27) can be adapted again to be applied for the small and big membranes, noticing that g_{ec} should be taken as the uniform weight of the girder in both membranes.

3.2.8 Self-anchored anchor cables

In a fully self-anchored cable-stayed bridge, the self-anchored anchor cable linked to the end pier commonly balances the pylon's bending moment which is induced by the different cable forces between the mid span and the side span. In the present study, the self-anchored anchor cable and its function are kept in the new cable-supported bridge model, whether the earth-anchored anchor cables are installed or not.

Considering the moment balance of the pylon in the region with self-anchored stay cables, the maximum force N_{bs} and material quantity for the self-anchored anchor cable Q_{bs} are derived as Eq. (28) and (29), respectively

$$N_{bs} = \frac{M_{bs}}{h_t + h_{sa}} \sqrt{1 + (\frac{h_t + h_{sa}}{l_{ac}})^2} \tag{28}$$

$$Q_{bs} = \frac{\gamma_c}{f_c} M_{bs} \left(\frac{l_{ac}}{h_t + h_{sa}} + \frac{h_t + h_{sa}}{l_{ac}} \right) \tag{29}$$

where M_{bs} is the maximum unbalanced bending moment in the pylon caused by the self-anchored parts, with the live load being imposed only in the mid span. Thus M_{bs} is expressed as

$$M_{bs} = \frac{1}{8}(g_{sc} + g_2 + p)l_{sc}^2 - \frac{1}{2}(g_{ac} + g_2)l_{ac}^2 + \frac{1}{6}Q_{sc}l_{sc} - \frac{1}{3}Q_{ac}l_{ac} \tag{30}$$

3.2.9 Earth-anchored anchor cables

The earth-anchored anchor cables are installed to balance the pylon's maximum bending moment M_{be} caused by the earth-anchored part. The bending moment is determined by

$$M_{be} = \frac{1}{8}(g_{ec} + g_2 + p)l_{ec}(2l_{sc} + l_{ec}) + \frac{1}{4}Q_{ec}(l_{sc} + l_{ec}) \tag{31}$$

Therefore, the maximum force T_{be} and material quantity for the earth-anchored anchor cables Q_{be} are expressed as

$$T_{be} = \frac{M_{be}}{h_t + h_{sa} + \frac{1}{2}h_{ea}} \sqrt{1 + (\frac{h_b}{l_b})^2} \tag{32}$$

$$Q_{be} = \frac{\gamma_c}{f_c} \frac{l_b}{h_t + h_{sa} + \frac{1}{2}h_{ea}} M_{be} \left[1 + (\frac{h_b}{l_b})^2 \right] \tag{33}$$

3.3 Pylons

The pylon is taken as a column only subjected to the axial force. It comprises two parts as shown in Fig. 4: the top part with the stay cables and with the height of h_{sa}+h_{ea}; and the bottom part without the stay cables and with the height of h_n+h_t. In the top part, the cross-sectional area is

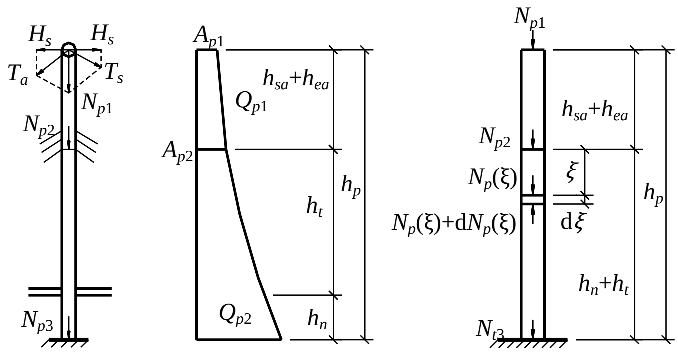

Fig. 4 Axial force and cross-sectional area in pylon

assumed to vary linearly along the height in which only the top and bottom sections reach the allowable stress of the material, while the bottom part is assumed as an equal strength column in which the stress reaches the allowable stress everywhere. This would simplify the calculation and would not cause unacceptable errors.

The axial force and cross-sectional area in the pylon are shown in Fig. 4. The axial force N_{p1} at the pylon's top is determined by the vertical component of the main cable force, which is expressed as follows

$$N_{p1} = \frac{(g_s + g_2 + 2Q_{sm}/l_m + 2Q_{hm}/l_s + p)l_s^2}{8h_s}\left(\frac{4h_s}{l_s} + \frac{h_c + 4h_a}{l_c}\right) \tag{34}$$

The axial force N_{p2} at the bottom of the top part is the sum of all of the loads over the section including the self-weight of the pylon, which is expressed as follows

$$\begin{aligned} N_{p2} &= (g_{ac} + g_2 + p)l_{ac} + (g_{sc} + g_2 + p)l_{sc}/2 + (g_{ec} + g_2 + p)l_{ec}/2 + Q_{ac} + Q_{sc} + Q_{ec} + N_{p1} \\ &\quad + Q_{p1} + \frac{M_{be}}{h_t + h_{sa} + \frac{1}{2}h_{ea}}\frac{h_b}{l_b} + \frac{M_{bs}}{l_a} \end{aligned} \tag{35}$$

where Q_{p1} is the material quantity for the top part, and it is expressed as

$$Q_{p1} = \frac{\gamma_p}{2f_p}(N_{p1} + N_{p2})(h_{sa} + h_{ea}) \tag{36}$$

Then N_{p2} can be obtained as

$$\begin{aligned} N_{p2} &= \Big\{(g_{ac} + g_2 + p)l_{ac} + (g_{sc} + g_2 + p)l_{sc}/2 + (g_{ec} + g_2 + p)l_{ec}/2 + Q_{ac} + Q_{sc} + Q_{ec} \\ &\quad + \left[1 + \frac{\gamma_p}{2f_p}(h_{sa} + h_{ea})\right]N_{p1} + \frac{M_{be}}{h_t + h_{sa} + \frac{1}{2}h_{ea}}\frac{h_b}{l_b} + \frac{M_{bs}}{l_a}\Big\} \Big/ \left[1 - \frac{\gamma_p}{2f_p}(h_{sa} + h_{ea})\right] \end{aligned} \tag{37}$$

In the bottom part, the axial force along the height can be found as Eq. (38) depending on the distance ξ to the top of the bottom part

$$N_p(\xi) = N_{p2}\exp(\frac{\gamma_p}{f_p}\xi) \tag{38}$$

The material quantity for the bottom part Q_{p2} can be obtained by subtracting N_{p2} from $N_p(h_n+h_t)$ calculated with Eq. (38), as follows

$$Q_{p2} = N_{p2}\{\exp[\frac{\gamma_p}{f_p}(h_n+h_t)]-1\} \tag{39}$$

Finally, the total material quantity for the pylon can be expressed as

$$Q_p = \frac{\gamma_p}{2f_p}(N_{p1}+N_{p2})(h_{sa}+h_{ea})+N_{p2}\{\exp[\frac{\gamma_p}{f_p}(h_n+h_t)]-1\} \tag{40}$$

3.4 Girders

The material quantity s for the girder Q_g and that for the superimposed structure Q_{g2} fare conveniently found by multiplying the uniformly distributed self-weight with the girder length as follows

$$Q_g = g_{as}l_{as}+g_{ac}l_{ac}+g_{sc}\,l_{sc}/2+g_{ec}\,l_{ec}/2+g_s\,l_s/2 \tag{41}$$

$$Q_{g2} = g_2(l_{as}+l_{ac}+l_{sc}/2+l_{ec}/2+l_s/2) \tag{42}$$

The uniformly distributed self-weight g_s and g_{as} in the suspension parts can be assumed as constant values because that the girder's axial force in these parts is a constant value. However, the uniformly distributed self-weight g_{ac}, g_{sc} and g_{ec} in the remaining parts need to be calculated carefully because of the accumulated axial force along the girder length.

As an example, the self-weight g_{sc} of the mid span self-anchored girder in Fig. 2 should meet

$$\frac{(f_g/\gamma_g)\mathrm{d}g_{sc}}{(g_{sc}+g_2+p)\mathrm{d}x} = \frac{x}{h_t+2h_{sa}\,x/l_{sc}} \tag{43}$$

With the initial condition that $g_{sc,lsc/2}$=0, the differential equation reaches the following solution

$$g_{sc}(x) = \left\{\exp\left[\frac{\gamma_g}{f_g}\frac{l_{sc}}{2h_{sa}}\left(\frac{l_{sc}}{2}-x+\frac{h_t l_{sc}}{2h_{sa}}\ln\frac{2x/l_{sc}+h_t/h_{sa}}{1+h_t/h_{sa}}\right)\right]-1\right\}(g_2+p) \tag{44}$$

It is too complicated to introduce Eq. (44) and the similar ones for other girder parts directly into the former equations. Furthermore, the initial condition of $g_{sc,lsc/2}$=0, which is the minimum value from Eq. (44), is not consistent with real bridges in practice. Therefore, the following semi-theoretical and semi-experiential formulas, Eq. (45)-(49), for the uniformly distributed self-weights are proposed by smooth curve fitting based on the values from several present long-span bridges or trial designs. It is noticed that the exponential function and the correlative parameters in Eq. (44) are still remained in the following formulas.

$$g_{sc}=\left\{0.6\exp\left[\frac{\gamma_g l_{sc}^2}{4f_g(h_t+h_{sa})}\right]+\frac{1650\gamma_g}{f_g}\right\}(g_2+p) \tag{45}$$

$$g_{ec}=\left\{0.6\exp\left[\frac{\gamma_g l_{ec}(l_{sc}+l_{ec})}{4f_g(h_t+h_{sa}+h_{ea})}\right]+\frac{1650\gamma_g}{f_g}\right\}(g_2+p) \tag{46}$$

$$g_{ac}=\left\{0.6\exp\left[\frac{\gamma_g l_{ac}(l_{sc}-l_{ac})}{f_g(h_t+h_{sa})}\right]+\frac{1650\gamma_g}{f_g}\right\}(g_2+p) \tag{47}$$

$$g_s=\max\left\{g_{ec},\min\left[g_{sc},\frac{3500\gamma_g}{f_g}(g_2+p)\right]\right\} \tag{48}$$

$$g_{as}=\min\left[g_{ac},\frac{3500\gamma_g}{f_g}(g_2+p)\right] \tag{49}$$

3.5 Anchorages and foundations

A correct calculation of the material quantity for the anchorage and foundations is of considerable complexity as their structures and dimensions depend not only on the reaction forces but also on the greatly varied geometrical conditions in different projects. In the present study, two simple ratios, k_a for the anchorages and k_f for the foundations, between the material quantities and the reaction forces are adopted.

Thus, the material quantity for the anchorages Q_a can be expressed as Eq. (50), in which T_a and T_{be} can be found in Eq. (17) and (32), respectively.

$$Q_a=k_a(T_a+T_{be}) \tag{50}$$

For the foundations, the reaction force N_{p3} at the pylon's bottom can be found by replacing ξ with h_n+h_t in Eq. (38)

$$N_{p3}=N_{p2}\exp[\frac{\gamma_p}{f_p}(h_n+h_t)] \tag{51}$$

The reaction force in the end pier is equal to the vertical force of the self-anchored anchor cable, which is found as

$$N_b=M_{bs}/l_a \tag{52}$$

Thus, the material quantity for the foundation Q_f is expressed as

$$Q_f=k_f(N_{p3}+N_b) \tag{53}$$

3.6 Bridge cost formula

The cost of the new model is obtained by substituting the material quantities obtained in section

Table 1 Varied parameters

Bridge types Parameters	Suspension bridge	Cable-stayed bridge	CSSB	PEACSB
l_a	l_a or 0	l_a	l_a	l_a
l_{ac}	0	l_a	l_a	l_a
l_{as}	l_a or 0	0	0	0
l_b	0	0	0	l_b
l_c	l_c	0	l_c	0
l_e	l_e	0	l_e	0
l_{ec}	0	0	0	l_{ec}
l_m	l_m	l_m	$l_s + l_{sc}$	$l_{ec} + l_{sc}$
l_s	l_m	0	l_s	0
l_{sc}	0	l_m	l_{sc}	l_{sc}
L	$2l_a + l_m$	$2l_a + l_m$	$2l_a + l_s + l_{sc}$	$2l_a + l_{ec} + l_{sc}$
h_a	h_a	0	h_a	0
h_b	0	0	0	h_b
h_c	h_c	0	h_c	0
h_{ea}	0	0	0	h_{ea}
h_n	h_n	h_n	h_n	h_n
h_p	$h_t + h_n$	$h_{sa} + h_t + h_n$	$h_{sa} + h_t + h_n$	$h_{ea} + h_{sa} + h_t + h_n$
h_{sa}	0	h_{sa}	h_{sa}	h_{sa}
h_t	h_t	h_t	h_t	h_t

3.2 to section 3.5 into Eq. (2), which is expressed as follows

$$C = 2[\mu_h(Q_{hm} + Q_{ha}) + \mu_s(Q_{sm} + Q_{sa}) + \mu_c(Q_{sc} + Q_{ac} + Q_{ec} + Q_{bs} + Q_{be}) \\ + \mu_p Q_p + \mu_g Q_g + \mu_{g2} Q_{g2} + \mu_a Q_a + \mu_f Q_f] \tag{54}$$

However, the parameters in the new bridge model as shown in Fig. 1 must be varied in order to calculate the cost for the four bridge types with Eq. (54). Then, the varied parameters for each bridge type are shown in Table 1.

4. Numerical examples

4.1 Parameters' values

In the following examples, the parameters' values adopted are shown in Table 2. These values are extracted from several in-service or under designing long-span bridges. It should be specially mentioned that two divisors are taken into account in the allowable stress of each material. The former divisor is the safety factor between the strength and the allowable stress. The latter one is an empirical factor to represent the effect of the bending moments in the structural members. Furthermore, the increased cost caused by the non-structural components and the construction is also taken into account in this empirical factor.

Table 2 Parameters

Parameter	Notation	Value
Bulk density of structural materials	γ_c, γ_g, γ_h, γ_s	78.5 kN/m^3
	γ_p	26.0 kN/m^3 (Concrete) 78.5 kN/m^3 (Steel)
Allowable stress of structural materials	f_c	1670 MPa/2.5/1.25=534.4MPa
	f_g	345 MPa/1.7/1.3=156.1MPa
	f_h	1670 MPa/4.0/1.25=334MPa
	f_p	19.25 MPa/1.0/3.15=6.11MPa
	f_s	1570 MPa/2.5/1.25=502.4MPa
Uniformly superimposed dead load	g_2	2.03 kN/m^2
Uniformly distributed live load	p	1.4 kN/m^2
Cost of unit weight of structural materials	μ_a	\$16/kN
	μ_c	\$480/kN
	μ_f	\$19/kN
	μ_g	\$320/kN
	μ_{g2}	\$80/kN
	μ_h	\$450/kN
	μ_p	\$24/kN
	μ_s	\$400/kN
Ratio for material quantity for anchorage	k_a	1.0 (in rock) 3.0 (on shore) 6.0 (in shallow water) 8.0 (in deep water)
Ratio for material quantity for foundation	k_f	1.8
Height from girder to main cable at bridge center	h_h	5.0
Anchoring zone height in pylon with self-anchored stay cables	h_{sa}	$l_{sc}/16$
Anchoring zone height in pylon with earth-anchored stay cables	h_{ea}	$l_{ec}/16$
Projection length of earth-anchored stay cables	h_b	$h_{ea}/2+h_{sa}+h_t+h_n$
	l_b	$\max(h_b/\tan30^{\circ}, l_a)$
Projection length of main cable in side-spans	h_c	$h_{ea}+h_{sa}+h_t$
	l_c	$\max(h_c/\tan30^{\circ}, l_a)$
Main cable length beyond the splay saddle	l_e	$0.1l_c$
Pylon height below girder	h_n	$\min(l_m/15, 70\text{ m})$

4.2 Verification examples

By using the formulas produced in section 3 and the parameters listed in Table 2, the costs of several long span bridges opened to traffic between 1998 and 2013 are calculated and listed in Table 3. The real costs of the main bridges, not including the approaching bridges, are available in literatures and listed in Table 3 after necessary currency changes.

In fact, the price of the materials and the construction cost of a bridge in different time and different country varies greatly. However, the exact values of the factors in Table 2 for the specific

Table 3 Comparison between calculated costs and real costs

No.	Type	Bridge Name	Main Span Length (m)	Deck Width (m)	Real Cost ($\times 10^6$ \$)	Calculated Cost ($\times 10^6$ \$)	Error
1	Suspension Bridge	Akashi-Kaikyo	1991	35.5	1916[a]	1357	-29.18%
2		East Great Belt	1624	31.0	620[b]	690	11.30%
3		Yi-Sunsin	1545	25.7	434[c]	531	22.38%
4		Hardanger	1310	20.0	298[d]	267	-10.59%
5	Cable-stayed Bridge	Sutong	1088	35.4	380[e]	351	-7.65%
6		Stonecutters	1018	39.0	356[f]	326	-8.55%
Average of the absolute values of errors							14.94%

a,b: Wiratman 1997; c: Virola 2010; d: Structurae 2014; e: Virola 2005; f: Wikipedia 2014.

bridge could hardly be found. Table 3 shows that the errors between the calculated costs and the real ones are normally lower than 30%, and the average error is 14.94%. This indicates that the formulas agree well with the real bridge from the viewpoint of estimation in the conceptual design stage.

5. Span limits

In a particular project, only the bridge type with sufficient span ability would be considered. Therefore, the span limit of each bridge type is vital in the conceptual design. To this end, the span limits of the four bridge types mentioned formerly are calculated and investigated in this section.

The ultimate condition of Eq. (13) and (21) is the value of them approaching infinity, based on the setting that the cables are only able to sustain their self-weight. Then, two equations are derived as follows

$$\frac{8h_s}{l_s} - \frac{\gamma_s}{f_s} l_s \sqrt{1+\left(\frac{4h_s}{l_s}\right)^2} = 0 \tag{56}$$

$$1 - \frac{\gamma_c l^2}{f_c (h_t + 2 h_{sa} x / l_{sc})} = 0 \tag{57}$$

The span limits of suspension bridges and cable-stayed bridges can be obtained from Eq. (56) and Eq. (57), respectively, as shown in the follows

$$l_{sus,\max} = \frac{8h_s}{l_s} \Bigg/ \left[\frac{\gamma_s}{f_s} \sqrt{1+\left(\frac{4h_s}{l_s}\right)^2} \right] \tag{58}$$

$$l_{cab,\max} = 1 \Bigg/ \left[\frac{\gamma_c}{f_c} \left(\frac{l_{cab}}{4h_{cab}} + \frac{h_{cab}}{l_{cab}} \right) \right] \tag{59}$$

A conclusion is found from Eq. (58) and (59) that the span limits of the two bridges, $l_{sus,\max}$ and

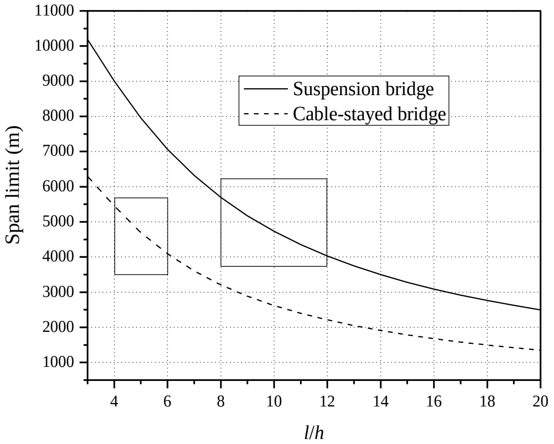

(a) Steel cable

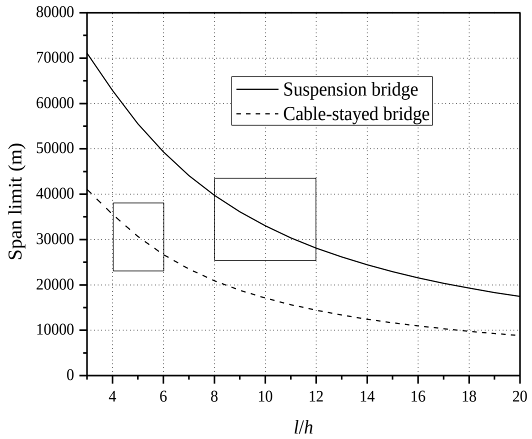

(b) CFRP cable

Fig. 5 Variation of span limits with span-to-height ratio

$l_{cab,\max}$, depend on the span-to-height ratio l_s/h_s or l_{cab}/h_{cab} and the density-to-strength ratio γ_s/f_s or γ_c/f_c. Generally speaking, the span-to-height ratio may vary from lower than 3 to over 15, whereas the density-to-strength ratio depends on the material type and is comparatively fixed, such as 78.5 kN/m^3 : (500 ~ 535)MPa for steel cables or 18.0 kN/m^3 : 800 MPa for CFRP cables.

The span limits of suspension bridges and cable-stayed bridges with steel cable and CFRP cable are shown in Fig. 5. A decreasing tendency with the increasing of the span-to-height ratio is obviously presented. It also can be seen that suspension bridges are superior to cable-stayed bridges, and CFRP cables are superior to steel cables.

In practice, the span-to-height ratio is generally between four and six for cable-stayed bridges as shown in the region indicated with a box in Fig. 5. The corresponding span limit is 5452 m to 4089 m with steel cables, but it can reach a much larger value of 35555 m to 26667 m with CFRP cables. However, the span-to-height ratio is approximately doubled as 8 to 12 in suspension bridges, and the corresponding span limit is 5697 m to 4028 m and 39752 m to 28109 m with steel cables and CFRP cables, respectively.

Lewis (2012) also proposed a model to assess the span limits for cable-stayed bridges and suspension bridges. However, Lewis takes a different allowable stress for cable steel as 700 MPa, while in this study these values are 502.4 MPa and 534.4 MPa for suspension bridges and cable-stay bridges, respectively. If the allowable stress were set to 700 MPa, the span limit of cable-stay bridges with the span-height ratio of 4 and 6 would rise to 7141 m and 5356 m, compared to 7000 m and 5250 m by Lewis, and the comparative difference is only 2.0%. For suspension bridges, the span limit would be 7944 m, which is 5.5% lower than 8411 m by Lewis with a span-height ratio of 8, and 5617 m with an error of 2.0% with the ratio of 12. In a word, the results match quite well.

The span limits for the new bridge model and CSSB are identical to that of suspension bridges. This is because that the bridge model is only able to carry the self-weight of the main cable when the theoretical span limit is reached. Both the new bridge model and the CSSB degrade to the same system with only the main cable. As the same reason, PEACSB's span limit is equal to that of cable-stayed bridges based on the same condition that the outermost cable only carries its self-weight. It should be mentioned that PEACSB's span capacity is much larger than that of cable-stayed bridges from the viewpoint of the girder's stability (Nagai *et al*. 2004), nevertheless this doesn't fall within the scope of this study.

6. Effect of cables' self-weight

In the material quantity formulas in section 3, the formulas are much simplified with the self-weight being neglected. Fig. 6 unfolds the comparative errors of the material quantities only in the cable system with the self-weight being not considered. Five bridge types, including cable-stayed bridges (CSBs), partially earth-anchored cable-stayed bridges (PEACSBs), triple span suspension bridges (TSSBs), single span suspension bridges (SSSBs) and cable-stayed-suspension bridges (CSSBs), are discussed.

It can be seen clearly that the errors are nearly proportional to the mid-span length. In the span range under 1000 m, the errors are around 10%, while they climb dramatically to 40%-75% at 5000 m. This will further bring about the increase in the material quantities of the other structural parts. As the span increases, the self-weight of the cable increases too and becomes more and more significant, which leads to the decrease of the bearing efficiency. This is also known as the so called "cable-sag effect". From this viewpoint, the researchers suggest that the self-weight could only be ignored with a mid-span under 800m if the acceptable errors were set to under 10%.

Fig. 6 also displays the comparison between different bridge types. With a mid-span under 1500m, cable-stayed-suspension bridges (CSSBs) have the lowest error, while cable-stayed bridges (CSBs) take the place over 1500m. On the other side, single span suspension bridges (SSSBs) and triple span suspension bridges (TSSBs) are always with the top two largest errors. This indicates that the stay cable system is superior to the suspension cable system in the viewpoint of bearing efficiency.

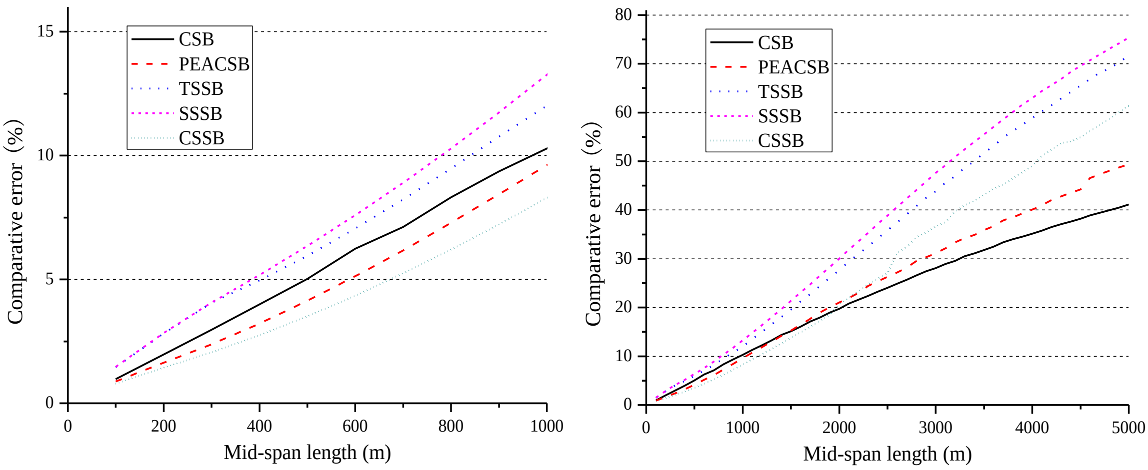

(a) Under 1000 m (b) 100 m-5000 m

Fig. 6 Comparative errors of the material quantities in the cable system

7. Geometrical parameters

For the new bridge model illustrated in Fig. 1, three key geometrical parameters controls the layout of the bridge model, and these parameters are investigated in this section. They are the ratio of earth-anchored girder length to mid-span length, the ratio of side span length to mid-span length, and the ratio of pylon's height to mid-span length. The three parameters are listed in Table 4. It should be especially mentioned that for the ratio of side span length to mid-span length in PEACSB and CSSB l_{sc} takes the place of l_m for the reason of practice custom, and only the pylon's height over the deck is included.

The mid-span of the bridge model may consist of two parts, including the self-anchored part (l_{sc}) and the earth-anchored part ($l_{ea} + l_s$). For the former part, the girder should be strengthened to accommodate the accumulated axial force. For the latter part, auxiliary structures, namely the anchorages, should be added to fix the cable system in side spans. As a balancing point, there should be an optimal division of the mid-span into the two parts. Therefore, the ratio of earth-anchored girder length to mid-span length in PEACSBs and CSSBs is investigated firstly.

As the first testing, the other two key parameters are assumed to be given values, the ratio of side span length to mid-span length (l_{ac}/l_{sc}) being 0.4 and the ratio of pylon's height to mid-span length ($(h_t + h_{sa} + h_{ea})/l_m$) being 0.2. The given values are among the suggested region for each key parameter, which will be illustrated later.

Figs. 7-8 illustrate the cost of PEACSB and CSSB under different ratio of earth-anchored girder

Table 4 Geometrical parameters in cable supported bridges

Parameters \ Bridge types	CSB	PEACSB	SSSB	TSSB	CSSB
Earth-anchored girder length to mid-span length	-	l_{ec}/l_m	-	-	l_s/l_m
Side span length to mid-span length	l_{ac}/l_m	l_{ac}/l_{sc}	-	l_{as}/l_m	l_{ac}/l_{sc}
Pylon's height over the deck to mid-span length	$(h_t + h_{sa})/\ l_m$	$(h_t + h_{sa} + h_{ea})/l_m$	h_t/l_m	h_t/l_m	$(h_t + h_{sa})\ l_m$

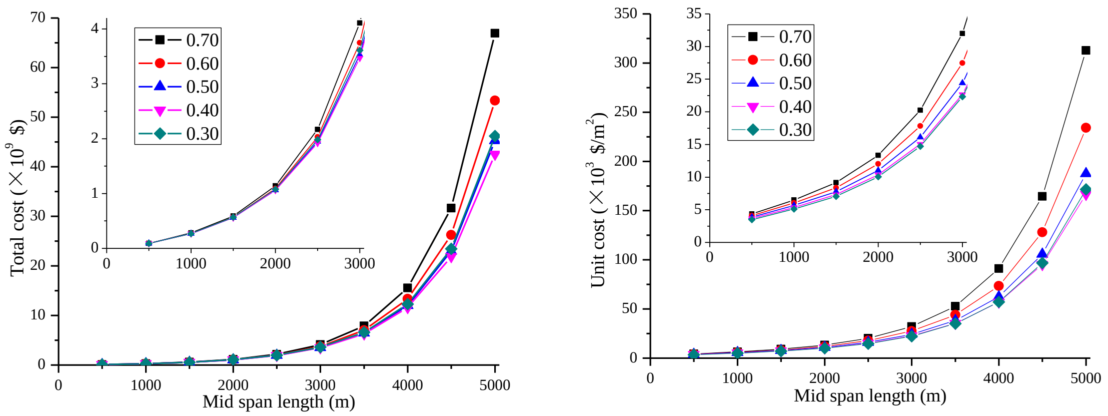

(a) Total cost (b) Unit cost per deck area

Fig. 7 Cost of PEACSB under different ratio of l_{ec}/l_m

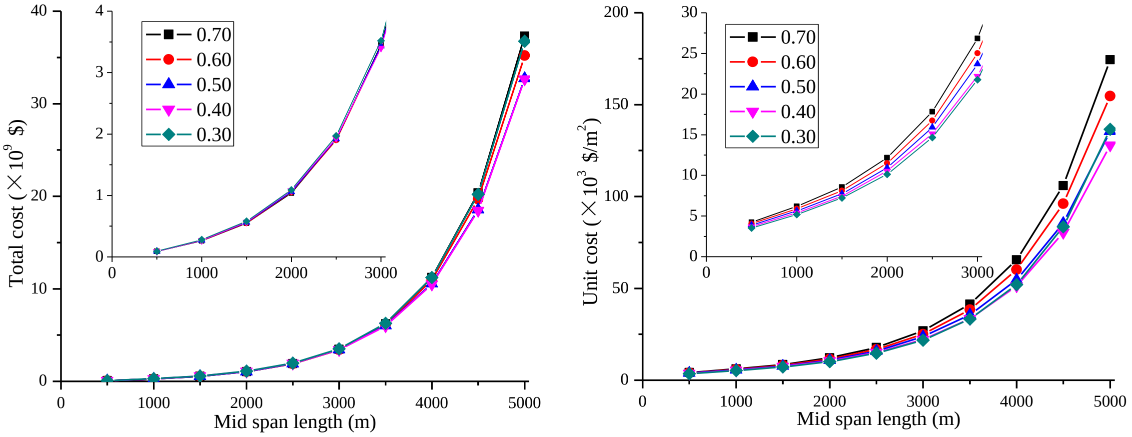

(a) Total cost (b) Unit cost per deck area

Fig. 8 Cost of CSSB under different ratio of l_s/l_m

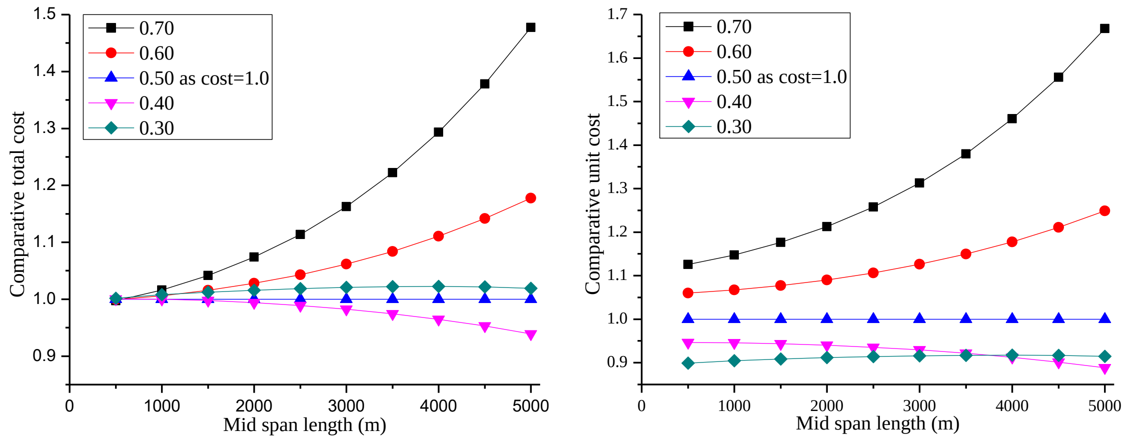

(a) Total cost (b) Unit cost per deck area

Fig. 9 Comparative cost of PEACSB under different ratio of l_{ec}/l_m

length to mid-span length, 0.3 to 0.7 with 0.1 intervals. It is no surprise that the cost experiences massive increase along all lines. Both the total costs and unit cost per deck area take the shape of exponential curves. A bridge with a mid-span length of 5000 m cost about 30-50 times to that of 1000 m-2000 m. Therefore, it is perfectly sensible to reduce the mid-span length at the premise of assuring the navigational clearance.

At the same time, it is very interesting to find that the lines of 0.3 and 0.4 are always at the bottom, or at least they are very close to other lines. In order to reveal the cost difference clearer, Figs. 9-10 show the comparative cost by setting the cost of 0.5 as cardinal numbers. The lines of 0.3 and 0.4 appear at the lower part of the graphs again. The cost saving are approximately 5-10 percent in most area, although sometimes the lines of 0.3 and 0.4 intersect with each other or even with that of 0.5.

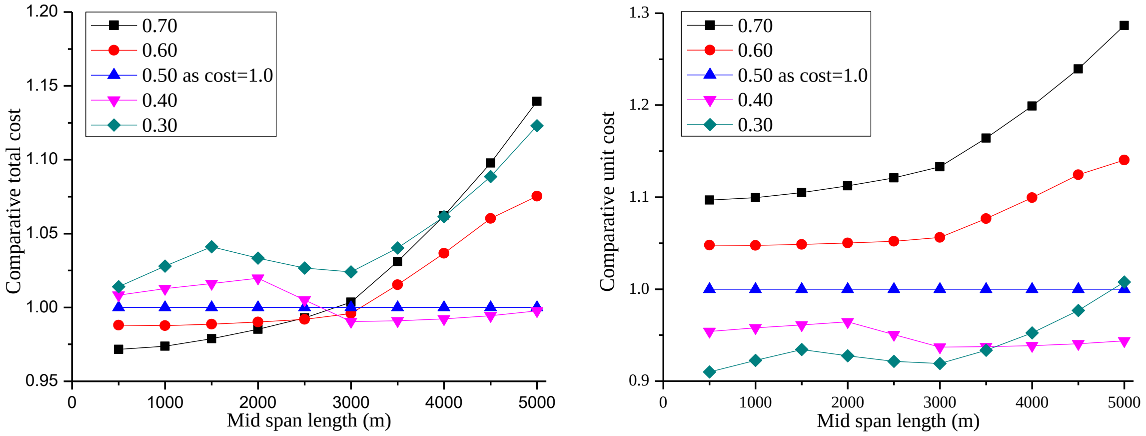

(a) Total cost (b) Unit cost per deck area

Fig. 10 Comparative cost of CSSB under different ratio of l_s/l_m

Table 5 Bridge type conversion under lowest total cost

Bridge types / Parameters	PEACSB	TSSB	CSSB
<1000 m	fully earth-anchored CSB 100% in Fig. 11(a)	SSSB 0% in Fig. 12(a) and Fig. 13(a)	SSSB 100% in Fig. 11(a)
1000-2400 m	normal	SSSB 0% in Fig. 12(a) and Fig. 13(a)	SSSB 100% in Fig. 11(a)
>2400 m	normal	SSSB 0% in Fig. 12(a) and Fig. 13(a)	normal

Table 6 Bridge type conversion under lowest unit cost per deck area

Bridge types / Parameters	PEACSB	CSSB
<800m	CSB 0% in Fig. 11(b)	CSB 0% in Fig. 11(b)
>800m	normal	normal

The other two ratios can be analyzed following the same rule. However, another method is taken in the following part to keep the paper concise. All three ratios are set as variables at the same time. Figs. 11-13 show the optimal values of the three ratios. The results can be analyzed in the following ways.

1. Some ratios equal 100% or 0%, or several lines may coincide with each other in particular span range. This means that the bridge type converts into another. Tables 5 and 6 lists such cases under the lowest total cost and unit cost per deck area, respectively. For example, Table 5 shows TSSB changes into SSSB. This is because that the SSSB and TSSB have equal mid span lengths and the cost of approaching spans are not included in the comparison. Therefore, the total cost of SSSB is lower than the TSSB for lacking of side spans. To acquire a comprehensive comparison result, the unit cost comparison are also discussed in this paper. Though the reason of the

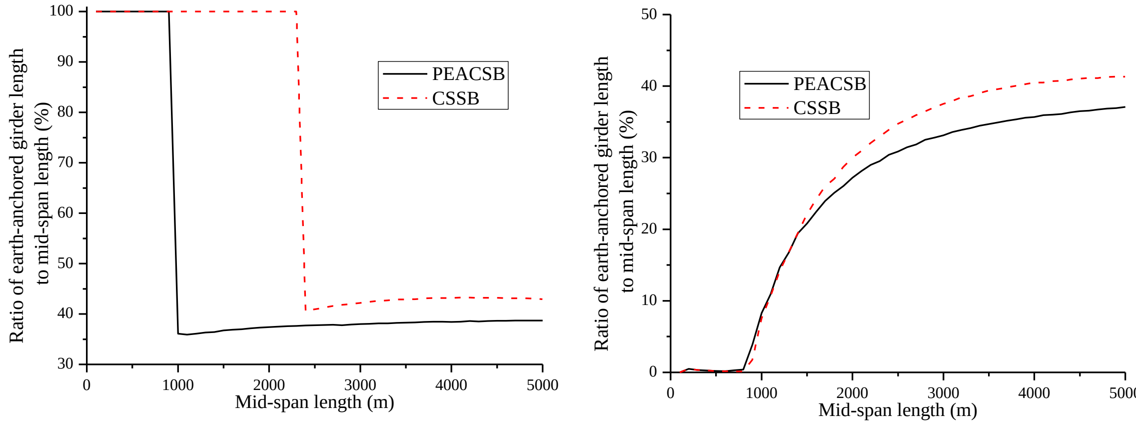

(a) Under lowest total cost (b) Under lowest unit cost per deck area

Fig. 11 Optimal ratio of earth-anchored girder length to mid-span length

conversion lies in the combination action of the three ratios, the sequence of different bridge costs is definitely various in different span ranges. This is to be discussed again in later sections.

2. As to the ratio of earth-anchored girder length to mid-span length, minimizing the total length of the bridge by decreasing the ratio is beneficial for the total cost, while it is just reverse for the unit cost per deck area. Therefore, the ratio starts with 100% and 0% in Figs. 11 (a)-(b), respectively. However, both in the two graphs the ratio approaches to about 35%-40% with the increase of the mid-span length. The ratio is less than 50%, which means that the self-anchored structure is economically superior to the earth-anchored structure with a large span length. The conclusion is that the suggested value for the ratio in practice is 35%-40%.

3. The ratio of side-span length to mid-span length increases with the mid-span length also. The suggested value is 40%-45% both for the total cost and the unit cost. Hassan (2013, 2014) also found that the cost of the bridge decreases almost linearly with the decrease of the ratio of main span length to bridge length, in other words, with the increase of the ratio of side span length to main span length. Lute (2009) found that the optimum value of the ratio of side span to main span is almost 0.4~0.5. However, those former researches only discussed within the bridge lengths under 700 m while this paper mainly concerns about long span bridges with span length over 1000m, and this extends the applicable scope of the conclusion. Besides the conversion shown in Table 5 and 6, the following two breaks in Fig 12 should be intentionally discussed. Under the lowest total cost, the ratio in PEACSB jumps from 30% to 45% at 2700 m. Under the lowest unit cost, the ratio in TSSB decreases from 35% to 22% and then jumps to 50% at 1000 m. With a shorter side-span, the cost of girder is certainly saved, while the cost of the anchorage increases with the increased inclination angel of the earth-anchored cables and the anchoring force lying in it, and vice versa. At a particular span length as indicated in Fig. 12, the comparison between the two trends reverses. In such cases, the lengthened side span is free of charge, of which can be intentionally utilized in practice.

4. The optimal ratio of pylon’s height to mid-span length drops sharply with a mid-span less than 1000 m and far less significant change takes place beyond 1000m. It remains as about 18% in CSB, with a corresponding inclining angle of the outmost stay cable in mid-span as about 20°. In other bridge types with anchorages, the pylon’s height must be decreased to minimize the inclining

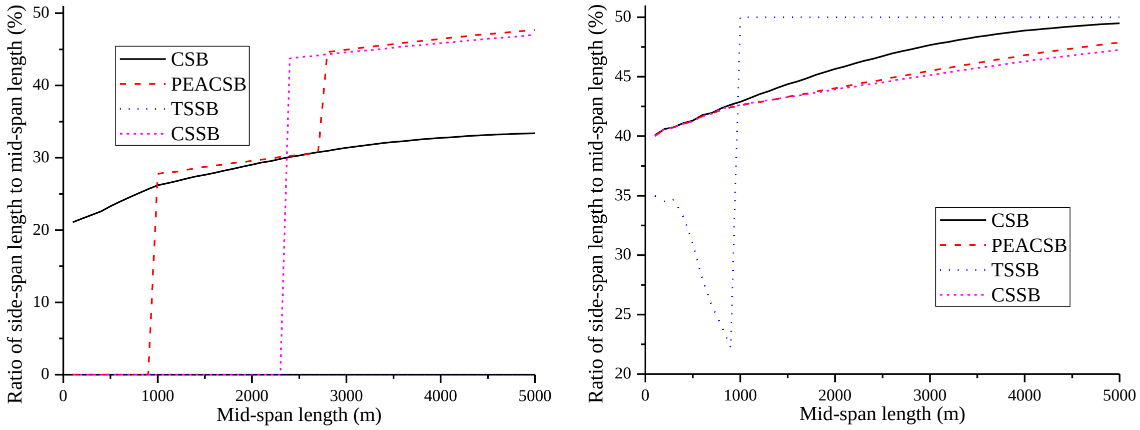

(a) Under lowest total cost (b) Under lowest unit cost per deck area

Fig. 12 Optimal ratio of side-span length to mid-span length

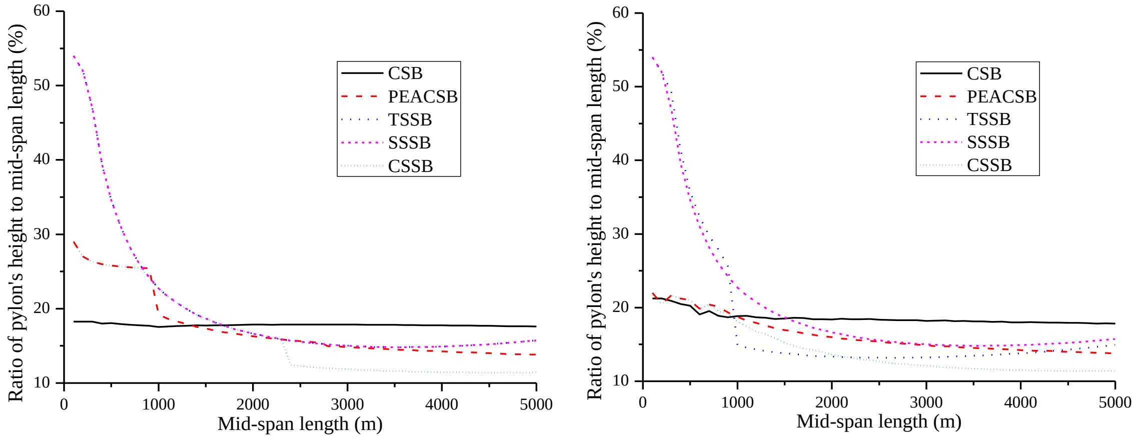

(a) Under lowest total cost (b) Under lowest unit cost per deck area

Fig. 13 Optimal ratio of pylon's height to mid-span length

angle of the cables, therefore the ratio is smaller as about 0.10 to 0.15, with a corresponding rise-to-span ratio of about 1/10 to 1/6 for main cables. These results are lower than the commonly believed values. For example, Gimsing (2012) reckon that 0.175 is the optimum value for suspension bridges with a 3000m main span, and Lewis (2012) suggested 0.125 for suspension bridges and 0.33 for cable-stay bridges. However, the former studies only paid attention to the cost of the cable systems and the pylons and neglected the anchorages and the foundations. Taking the substructure into account, the suggested value is 18% for CSB and 15% for other bridge types.

8. Costs of different bridge types

8.1 Comparison between the bridge types

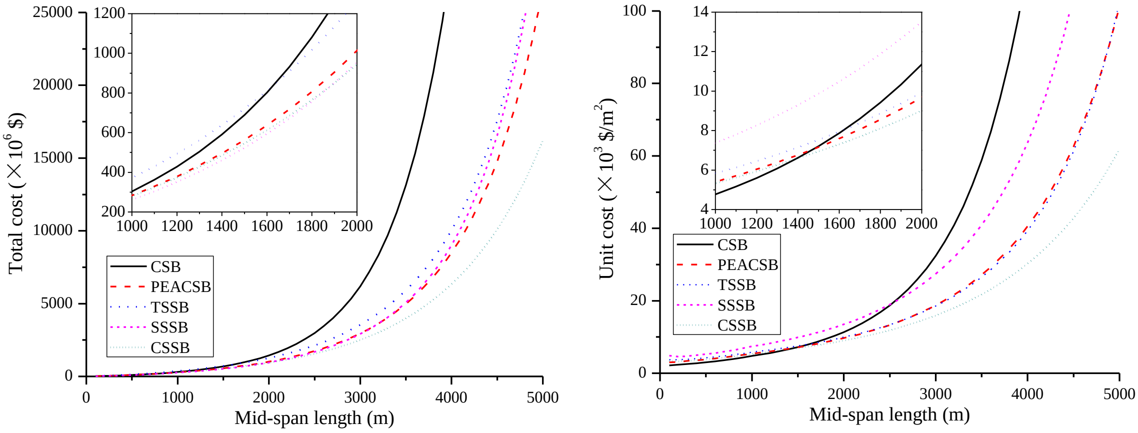

(a) Total cost (b) Unit cost per deck area

Fig. 14 Costs of the five bridge types

It's of the same importance to discuss the cost of the bridge as the optimal value of the geometrical parameters. However, if the optimal values obtained in section 3 were adopted, the costs of each bridge type would be very close to each other, and even conversions as shown in Tables 5 and 6 between bridge types would take place. These results are intentionally omitted here.

Fig. 14 displays the total costs and unit costs per deck area of the five bridge types under same geometrical parameters as suggested in section 3. These parameters are: 40% for the ratio of earth-anchored girder length to mid-span length, 40% for ratio of side-span length to mid-span length, and 18% for the ratio of pylon's height to mid-span length in CSB and 15% in other bridge types. Under this premise, the CSB has the same total length as the TSSB, while the PEACSB is same as the CSSB. The SSSB is the shortest one because only the mid-span exists.

For the total cost, CSB is the most economical bridge type with a mid-span under 300m, and then SSSB take the place between 400m and 1800m because it has the least total bridge length. Lastly, CSSB has advantage over other bridge types beyond 1900 m by combining the advantages of the cable-stayed parts and the suspension parts. At the other end, TSSB has the highest cost under 1600 m, and then CSB becomes the most expensive one because it is approaching its span limit, about 4000 m to 5000 m as discussed in former part.

For the unit cost per deck area, several changes occur. The CSB is superior to other bridge types under 1300 m, and then CSSB takes the place. The SSSB is the most expensive one under 2500 m, while the CSB jumps from the lowest one under 1300 m to the highest one over 2600 m.

A quantitative comparison is also performed between 600 m and 2000 m as shown in Table 7 by setting the average cost of the five bridge types as the reference value. The span range is the most common and feasible area in practice nowadays. To make it clear, the lowest value is indicated with an underlining format, while the highest one is with a bar overhead. It is very clear that all bridge type experience a decreasing cost except the CSB.

For the total cost, the CSB experience the most dramatic increase from saving about 7% to wasting about 29%. The PEACSB's performance becomes better and better by saving about 5% to 10%. The TSSB cuts down its disadvantage from 28% to 12%, while the SSSB is the most economical one in most cases by saving about 12% to 15%, only that the CSSB becomes the most preeminent bridge type by promoting its saving from 5% to 16%.

Table 7 Bridge costs between 600 m and 2000 m

Mid-span	Total cost					Unit cost per area				
	CSB	PEACSB	TSSB	SSSB	CSSB	CSB	PEACSB	TSSB	SSSB	CSSB
600 m	0.933	0.954	$\overline{1.284}$	$\underline{0.880}$	0.949	$\underline{0.763}$	0.949	1.049	$\overline{1.295}$	0.943
800 m	0.972	0.951	$\overline{1.262}$	$\underline{0.875}$	0.940	$\underline{0.796}$	0.946	1.033	$\overline{1.289}$	0.936
1000 m	1.013	0.944	$\overline{1.241}$	$\underline{0.871}$	0.931	$\underline{0.830}$	0.941	1.017	$\overline{1.284}$	0.928
1200 m	1.057	0.937	$\overline{1.218}$	$\underline{0.867}$	0.921	$\underline{0.867}$	0.935	0.999	$\overline{1.280}$	0.919
1400 m	1.106	0.930	$\overline{1.195}$	$\underline{0.863}$	0.908	0.908	0.929	0.981	$\overline{1.275}$	$\underline{0.907}$
1600 m	1.161	0.922	$\overline{1.172}$	$\underline{0.859}$	0.886	0.955	0.922	0.964	$\overline{1.272}$	$\underline{0.887}$
1800 m	$\overline{1.221}$	0.912	1.149	$\underline{0.855}$	0.864	1.006	0.914	0.947	$\overline{1.268}$	$\underline{0.865}$
2000 m	$\overline{1.286}$	0.901	1.124	0.850	$\underline{0.839}$	1.062	0.904	0.928	$\overline{1.263}$	$\underline{0.843}$

For the unit cost, the CSB is the most economical one under 1200 m, while it converts to the other side over 1600 m. The PEACSB is again more and more economical by saving 5% to 10%. The TSSB reverses from over cost 5% to saving 7%, the SSSB is always the most expensive one by wasting 30% to 26%. The CSSB gradually stands out by saving 6% to 16%, and it is the best one over 1400 m.

Overall, the CSB's economic performance becomes deteriorative, while the bridge types with suspension parts are just on the contrary. Especially the bridge type combining the advantages of both the cable-stayed parts and the suspension parts, the CSSB and PEACSB, show their potential to stand out with a super long span length. Therefore, the two bridge type will be inevitably prosperous in future practice.

Another factor must be considered in the chosen of bridge types is the topography where the project is located. If no side spans were needed in a severe rugged topography, the total cost would play the most important role, and the SSSB should be paid more attention under 2000 m. While the topography is mild with a broad water or valley area, the CSB will definitely become the best one under 1600 m.

8.2 Cost of structural parts

Fig. 15 illustrates the cost proportions of the five parts, cables, pylons, girders, anchorages and foundations. The percentage of the girders and anchorages decreases, whereas that of the pylons and foundations increases, and that of the cables increases then decrease. The overall trend is that the proportion of the superstructure becomes less with the increase of the mid-span length. The cost of superstructure, including the cables, pylons and girders, is about 45%-60% of the total cost, which means that of the substructure is about 40%-55%. Between 600 m and 2000 m, the average proportions of the five structural parts are as follows: 15% for cables, 13% for pylons, 30% for girders, 15% for anchorages and 27% for foundations.

Several rules are found in the comparison of each bridge parts between different bridge types. The CSB has the lowest proportion of the cables, which means that the stayed cable system is more efficient than the suspension cable system. The CSB has the highest proportion of the girders, for that the girders are under huge compressive forces and the cross sectional area must be enlarged all along the span. The PEACSB and CSSB enjoy less anchorage proportion than the

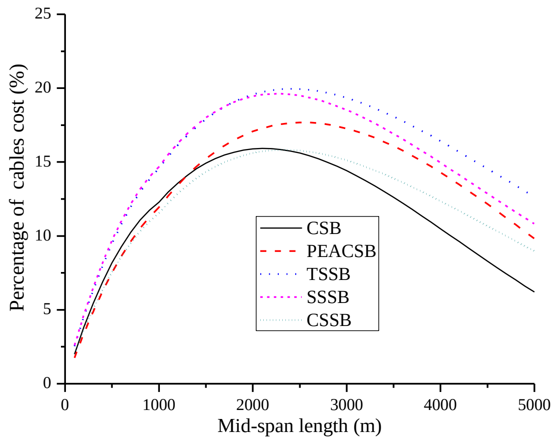

(a) Cables

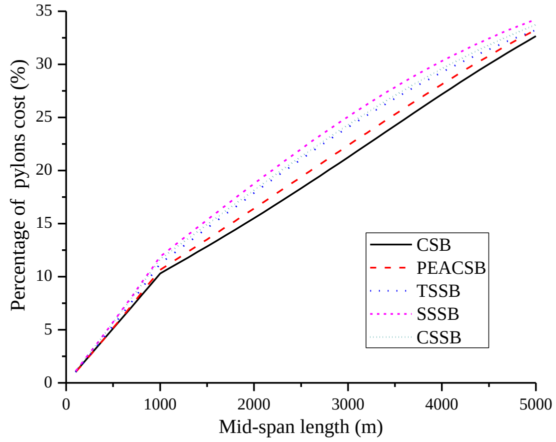

(b) Pylons

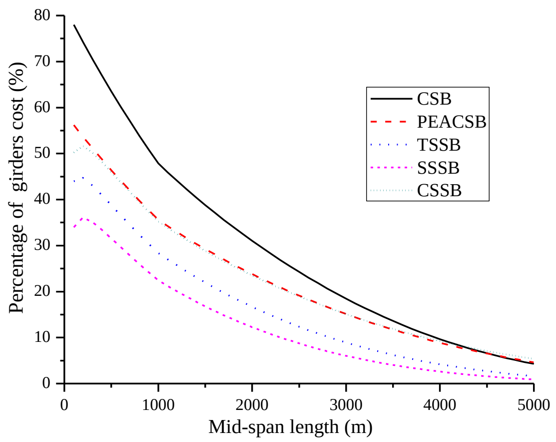

(c) Girders

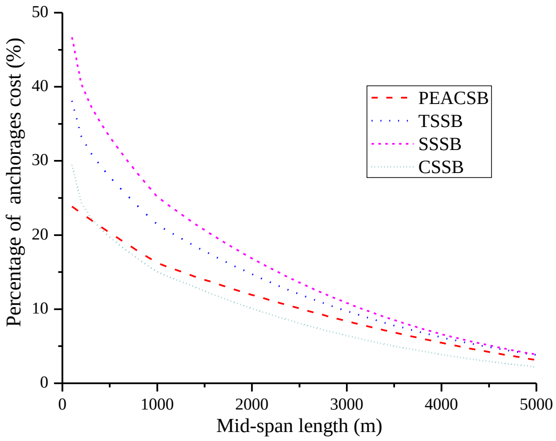

(d) Anchorages

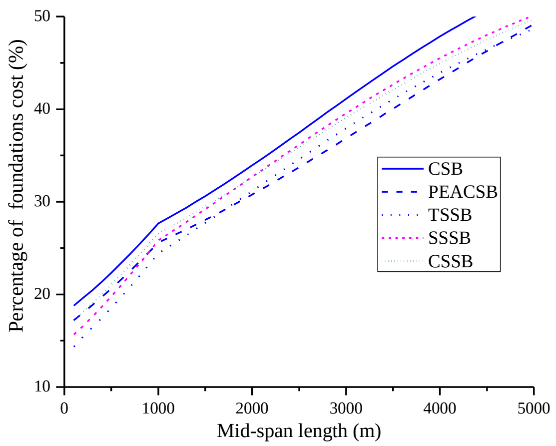

(e) Foundations

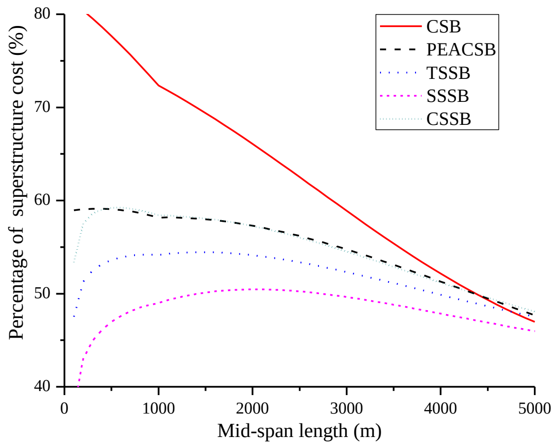

(f) Superstructure

Fig. 15 Proportion of structural parts

TSSB and SSSB, which embodies the advantages of the combination of the earth-anchored and self-anchored structures.

9. Effect of geological conditions

The geological condition has great influence on the costs of the anchorage and the foundation. Based on the geological conditions, anchorages can be divided into gravity anchorages and rock socketed anchorages. As a step further, the terrain conditions for the gravity anchorages can be classified into three types, including on shore, in shallow water and in deep water. Investigations show that the anchorage ratio k_a for rock socketed anchorages, gravity anchorage on shore, in shallow water and in deep water have values as 1.0, 3.0, 6.0 and 8.0, respectively, and the ratio k_f for the foundations have values as 1.8 on the shore, 3.6 in shallow water and 4.8 in deep water, respectively.

The parametric study mentioned above assumes that the bridge is on shore. There is no doubt that the various geological conditions will directly affect the costs of the anchorage and the foundation, so as to the optimal parameters of the structure.

The interaction among the three geometric parameters discussed in section 3 is so significant that the influence of the geological conditions would be confused. Therefore, the three parameters are studied separately again as that in section 4. Further comparison reveals that the effect of geological conditions on the ratio of side span length to mid-span length is about 2%, compared to that of pylon's height over the deck to mid-span length is about 5%. However, the influence on the ratio of earth-anchored girder length to mid-span length is the largest, which is intentionally presented below. Now the ratio of side-span length to mid-span length is set as 40%, and the ratio of pylon's height to mid-span length is 18% for CSB and 15% for other bridge types.

Fig. 16 illustrates that the optimal ratios of earth-anchored girder length to mid-span length of PEACSB and CSSB increase with the geological condition getting better.

For a hybrid structure with earth-anchored and self-anchored parts, the deterioration of geological condition would lead to the rise of anchorage cost and inevitably reduce the length of

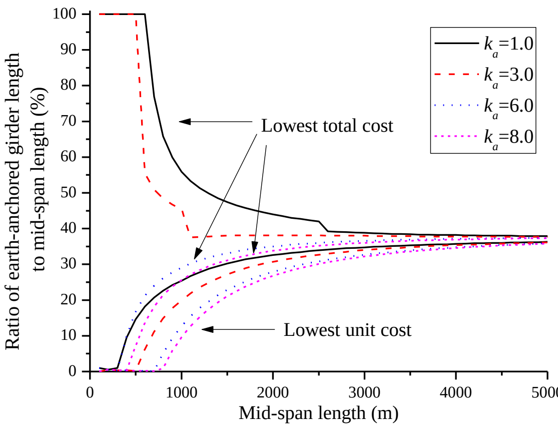

(a) PEACSB

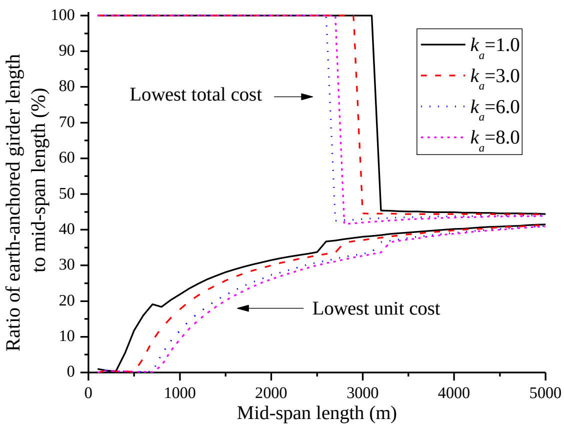

(b) CSSB

Fig. 16 Optimal ratio of earth-anchored girder length to mid-span length in four geological conditions

Table 8 Optimal ratio of earth-anchored girder length to mid-span length under four geological conditions

Bridge type	Mid-span Length (m)	Ratio of earth-anchored girder length to mid-span length (%)							
		Under lowest total cost				Under lowest unit cost			
		Rock	Shore	Shallow Water	Deep Water	Rock	Shore	Shallow Water	Deep Water
PEACSB	1000	55.90	45.50	29.10	25.60	25.40	19.90	12.70	9.60
	1500	47.40	38.00	33.13	31.13	30.20	27.20	22.87	21.07
	2000	43.95	38.10	35.00	33.75	32.55	30.70	27.90	26.80
CSSB	1000	100.00	100.00	100.00	100.00	21.90	17.70	11.80	9.30
	1500	100.00	100.00	100.00	100.00	28.07	25.67	21.73	20.13
	2000	100.00	100.00	100.00	100.00	31.45	30.00	27.25	26.10

earth-anchored part. The difference is obvious between the optimal ratios under four geological conditions at the beginning of the curves. For example, the optimal ratio of PEACSB ranges from 10% to 60% under different conditions with a mid-span length of about 1000 m. As the span increases, the advantage gradually decreases, and eventually the optimal ratios are all about 40% for both PEACSB and CSSB and under all geological conditions. This is because the difficulties and costs in both the self-anchored part and earth-anchored part are getting higher with the increase of the span length, and it will gradually become the dominant factor over the cost of the anchorages.

Table 8 compares the optimal ratios under the four kinds of geological conditions of PEACSB and CSSB with a mid-span length range of 1000m to 2000m which is widely adopted in practice. The difference between the optimal ratios of PEACSB and CSSB is approximately 25% with a 1000 m mid-span length, while it decreases to about 10% with the span increasing to 2000 m. These rules and values will be very useful in future engineering practice.

10. Optimization of new bridge model

In this section, the degradation of the new bridge model is no longer concerned, which means that the bridge model proposed in this study will not be varied to four kinds of bridge types mentioned above. The length of self-anchored cable-stayed parts l_{sc}, the length of earth-anchored cable-stayed parts l_{ec}, and that of the suspension part l_s could be changed freely, so that the combination of the three bridge structural parts is optimized in the viewpoint of lowest cost.

For the bridges with a mid-span length of 100-7500m, the optimized percentages of the three parts are shown in Fig. 17, with the ratio of side-span length to mid-span length (l_{ac}/l_{sc} and l_{ac}/l_s) being set as 40% and the ratio of pylon's height to mid-span length being set as 15% in the model.

It can be clearly seen that the self-anchored cable-stayed part is alsways the dominant part with the consideration of either the lowest total cost or the lowest unit cost. This certifies again that the self-anchored cable-stayed strucutue is the best choice in the viewpoint of cost.

Fig. 17(a) displays the percentage of each structural parts with the lowest total cost. With a mid-span length less than 1000 m, the length of self-anchored cable-stayed part decreases sharply while the other two parts increase rapidly, and the length of earth-anchored cable-stayed part is

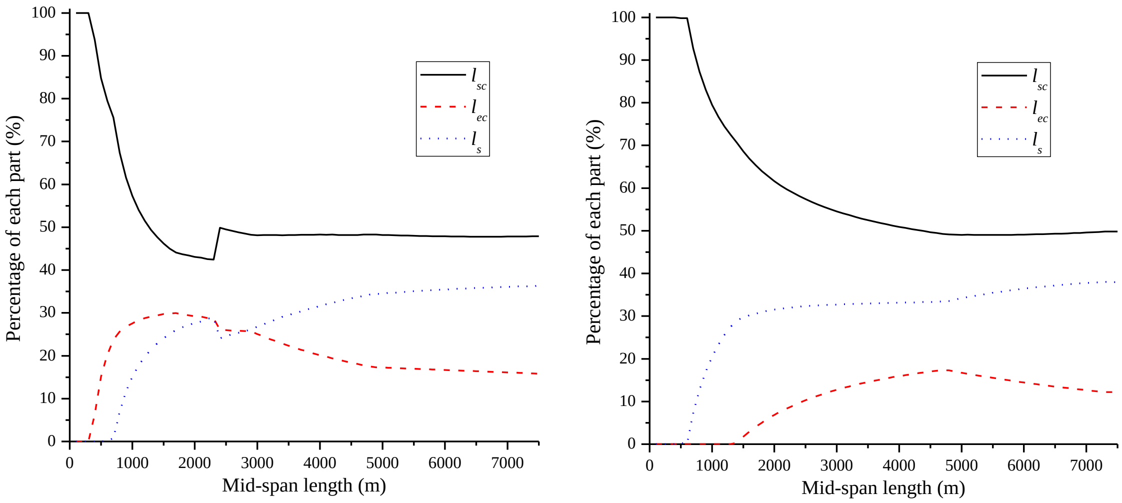

(a) Lowest total cost (b) Lowest unit cost

Fig. 17 Percentage of each structural part with lowest cost

larger than that of the suspension part. While the span is beyond 1000 m, the proportion of each part remains almost steady, but the contrast between the earth-anchored cable-stayed part and the suspension part reverses when the span is nearly 2500 m. That is to say, the economic performance of the earth-anchored cable-stayed structure is better than that of the suspension structure, but the comparison is reversed after the span is larger than 2500 m. After the span reaches 5000 m, the portions tend to be flat, and the percentage of self-anchored cable-stayed part, the earth-anchored cable-stayed part and the suspension part is stably about 48%, 16% and 36%, respectively.

Fig. 17(b) displays the percentage of each structural parts with the lowest unit cost. The self-anchored cable-stayed structure is more advantaged, and its ratio experiences little change while the mid-span grows to more than 5000 m, which is about 49%. On the other hand, the percentage of the earth-anchored cable-stayed part is smaller than that of the suspension part, which are 13% and 38%, respectively, after the span of 3000 m. There is no reversed correlation between the earth-anchored cable-stayed part and the suspension part as that with the lowest total cost, because the earth-anchored cable-stayed structure does not require side spans, and thus it is not advantaged while the cost is averaged by the total length.

In a word, the best way to achieve the most excellent economic performance is to combine the three types of structures in long span cable supported bridges.

11. Conclusions

In the present study, the formulas for the materials and the cost for cable-supported bridges are proposed, which can be applied to SB, CSB, CSSB, and PEACSB by using different parameters. Numerical examples for using the formulas for several bridges around the world are presented and the results show that the calculated results match well with those in the literature. The span limits of these bridges are calculated and investigated, as well. Finally, a parametric study is illustrated aiming at the relations between three key geometrical parameters and the cost of the bridge model.

This study can be summarized as follows:

• The formulas for material and cost estimation of the new bridge model are proposed based on the assumption that the stress in all of the bridge's members is equal to the allowable stress of the material. The formulas could be easily used in engineering practices.

•The estimated results from the model match well with those in the literature for many cable supported bridges.

•The span limits of SB and CSB depend on the span-to-height ratio and the density-to-strength ratio. The span limits of the new bridge model and CSSB are the same as that of SB, and the span limit of PEACSB also is equal to that of CSB, at the viewpoint of cable strength.

•Based on the assumption of the cable to support its self-weight, the span limit for SB with steel cables and CFRP cables is 5697 m to 4028m and 39752 m to 28109 m for different span-to-height ratios, respectively. For comparison, the corresponding span limit for CSB with steel cables and CFRP cables is 5452 m to 4089m and 35555 m to 26667 m for different span-to-height ratios, respectively.

• The comparative errors of the material quantity in the cable system without the self-weight being considered are nearly proportional to the mid-span length. The self-weight could only be ignored with a mid-span less than 1000 m if the acceptable errors were set to less than 10%.

•For bridges with earth-anchored parts, a decrease of the ratio of earth-anchored girder length to the total mid-span length cuts down the total cost and raises the unit cost per deck area. The suggested ratio in practice is 35%-40%.

• The optimal ratio of side-span length to mid-span length increases with the mid-span length. The suggested value is about 40%-45% in most span range.

• The optimal ratio of pylon's height to mid-span length drops sharply with a mid-span length less than 1000 m, and remains steady with a mid-span length over 1000 m. The suggested value is 18% for CSB and 15% for other bridge types.

•As the mid-span length grows, CSB's economic performance deteriorates but SB is just on the contrary. The CSSB and PEACSB which combines the advantages of both the earth-anchored structures and self-anchored structures show their potential to stand out with a super long span length.

• The percentage of the cost of the girders and anchorages decreases, whereas those of the pylons and foundations increase and that of the cables increases then decrease with the increase of the mid-span length.

• The geological conditions have the largest influence on the ratio of earth-anchored girder length to mid-span length, while the influence is little on the other two geometrical parameters.

• The self-anchored cable-stayed part is always the dominant part with the consideration of either the lowest total cost or the lowest unit cost. It is advisable to combine all three types of structures in long span cable supported bridges to achieve the most excellent economic performance.

Acknowledgments

The authors appreciate the financial support from the National Basic Research Program of China (973 Program) (Project No. 2013CB036303) and the National Natural Science Foundation of China (Project No. 51008223). The opinions and statements do not necessarily represent those of the sponsors.

References

Eamon, C.D., Jensen, E.A., Grace, N.F. and Shi, X. (2012), “Life-cycle cost analysis of alternative reinforcement materials for bridge superstructures considering cost and maintenance uncertainties”, *J. Mater. Civil Eng.*, **24**(4), 373-380

Gimsing, N.J. and Georgakis C.T. (2012), *Cable Supported Bridge: Concept and Design*, 3rd Edition, John Wiley & Sons, Chichester, UK.

Hassan, M.M., Damatty, E.A. and Nassef, A.O. (2014), “Database for the optimum design of semi-fan composite cable-stayed bridges based on genetic algorithms”, *Struct. Infrastr. Eng.*, **11**(8), 1054-1068.

Hassan, M.M., Nassef, A.O. and Damatty, E.A. (2013), “Optimal design of semi-fan cable-stayed bridges”, *Can. J. Civ. Eng.*, **40**, 285-297.

Lewis, W.J. (2012), “A mathematical model for assessment of material requirements for cable supported bridges: implications for conceptual design”, *Eng. Struct.*, **42**(9), 266-277.

Lute, V., Upadhyay, A. and Singh, K.K. (2009), “Computationally efficient analysis of cable-stayed bridge for GA-based optimization”, *Eng. Appl. Artif. Intel.*, **22**, 750-758.

Mara, V., Haghani, R., Sagemo, A., Storck, L. and Nilsson, D. (2013), “Comparative study of different bridge concepts based on life-cycle cost analyses and lifecycle assessment”, *Proceedings Of The 4th Asia-Pacific Conference On FRP In Structures, APFIS 2013*, Melbourne, December

Nagai, M., Fujino, Y., Yamaguchi, H. and Iwasaki, E. (2004), “Feasibility of a 1400 m Span Steel cable-stayed bridge”, *J. Bridge Eng.*, **9**(5), 444-452.

Safi, M., Sundquist, H., Karoumi, R. and Racutanu, G. (2012), “Integration of life-cycle cost analysis with bridge management systems”, *Tran. Res. Record*, **2292**, 125-133

Shao, X., Hu, J., Deng, L. and Cao, J. (2013), “Conceptual design of superspan partial ground-anchored cable-stayed bridge with crossing stay cables”, *J. Bridge Eng.*, **19**(3), 06013001.

Structurae (2014), http://structurae.net/structures/hardanger-bridge (Dec. 1, 2014).

Sun, B., Cheng, J. and Xiao, R.C. (2010), “Preliminary design and parametric study of a 1400 m partially earth-anchored cable-stayed bridge”, *Sci. China Ser. E: Technol. Sci.*, **53**(2), 502-511.

Tang, M.C. (2007), “Evolution of bridge technology”, *IABSE Symposium: Improving Infrastructure Worldwide*, Weimar, Germany.

Thoft-Christensen, Palle (2012), “Infrastructures and life-cycle cost-benefit analysis”, *Struct. Infrastr. Eng.*, **8**(5), 507-516

Virola, J. (2005), “Three long-span cable-Stayed bridges in China”, http://koti.kontu.la/jvirola/koti/PDF/sut2-pt.pdf (Dec. 1, 2014).

Virola, J. (2010), “The Gwangyang 1545 Bridge - great suspension bridge in South Korea”, http://koti.kontu.la/jvirola/koti/Gwangyang/ria-gwangyang.pdf (Dec. 1, 2014).

Wang, C.S., Zhai, M.S., Li, H.T., Ni, Y.Q. and Guo, T. (2015) “Life-cycle cost based maintenance and rehabilitation strategies for cable supported Bridges”, *Adv. Steel Constr.*, **11**(3), 395-410

Wang, X. and Wu, Z.S. (2010a), “Integrated high-performance thousand-metre scale cable-stayed bridge with hybrid FRP cables”, *Compos. Part B*, **41**(2), 166-175.

Wang, X. and Wu, Z.S. (2010b), “Evaluation of FRP and hybrid FRP cables for super long-span cable-stayed bridges”, *Compos. Struct.*, **92**, 2582-2590.

Wikipedia (2014), http://en.wikipedia.org/wiki/Stonecutters_Bridge (Dec. 1, 2014).

Wiratman, W. (1997), “Advanced suspension bridge technology and the feasibility of the Sunda Strait Bridge”, http://www.wiratman.co.id/ximages/sunda.pdf (Dec. 1, 2014).

Xiong, W., Cai, C.S., Zhang, Y. and Xiao, R. (2011), “Study of super long span cable-stayed bridges with CFRP components”, *Eng. Struct.*, **33**, 330-343.

Zhang, F.J., Nie, L.L. and Cao, H.Y. (2014), “Static deformational behaviors of cable-stayed suspension bridge and its simplified material cost model”, *Appl. Mech. Mater.*, **501-504**, 1221-1227.

Zhang, L., Xiao, R., Sun, B., Jiang, Y., Zhang, X., Zhuang, D., Zhou, Y. and Tu, X. (2013b), “Study on economic performances of multi-span suspension bridges part 2: Parametric study”, *Struct. Eng. Mech.*,

47(2), 287-305.
Zhang, R.X., Sun, B., Jiang, Y., Zhang, X., Zhuang, D., Zhou, Y. and Tu, X. (2013a), "Study on economic performances of multi-span suspension bridges part 1: Simple estimation formulas", *Struct. Eng. Mech.*, **47**(2), 265-286.

CC